King Fahd University of Petroleum & Minerals

Systems Engineering Department

**Term 071**

SE 514: Optimal Control

*Term Project*

# Optimal Control of Robotic Wheelchair

By

Mohammad Shahab (ID. 227598)

For

Prof. Magdi S. Mahmoud

Abstract

In this report, Optimal Control is applied to a Robotic Wheelchair. The report will review the original project of robotic wheelchair control. A detailed study of the mathematical model of the robotic wheelchair system will also be included. Then, Optimal Control will be investigated by applying several design concepts with detailed comments about each design applied. A conclusion of the work will end the report giving future recommendations and comments.

# Table of Contents

# 0. Introduction

Modern control strategies impacted many applications in many disciplines. One of these is the Optimal Control designs which pioneered in the early 60's of the 20th century.

In this report, Optimal Control is applied to a Robotic Wheelchair. The report will review the original project of robotic wheelchair control. A detailed study of the mathematical model of the robotic wheelchair system will also be included. Then, Optimal Control will be investigated by applying several design concepts with detailed comments about each design applied. A conclusion of the work will end the report giving future recommendations and comments.

# 1. Original Project Overview

In this section of the report, first, brief discussion of original project and work that is done in Kanagawa Institute of Technology will be presented. Secondly, the specific part of the project studied here is discussed. Final part of this section will be designated for the explanation of the robotic wheelchair mechanism.

## 1.1. Original Work

The main purpose of the project is to assist aged (old) individuals supporting themselves in using wheelchairs. Regularly, for a person using a wheelchair, the road or path the wheelchair maneuver through could include bumps or steps. Even if the step to be climbed is small, an old person ability to get over it most probably will need a assisting.

This work is presented in the paper by (Takahashi, et al., 2000). Other work related to the work can be found in (Takahashi, et al., 2005) and (Takahashi, et al., 2003).

Basically, the proposed system goal is assist the wheelchair user to be able to climb up an about 10 cm step without help. The proposed system consists of two stages of step climbing. First, front wheel rising is done. Secondly, after raising the wheelchair, an inverse pendulum control is applied. In order to firstly obtaining the front wheel rising, wheelchair's rear wheel shaft position is moved using a small force. When a person raises the wheelchair, a quick rising is expected. The force required to raise the front wheel 10 cm is inversely proportional to the rear wheel shaft position. So, a mechanical sliding of rear wheel shaft to change position for about 50 mm is set when a rising mechanism is applied. (Takahashi, et al., 2000)

After completing the part of front wheel rising of the wheelchair, the system enters the inverse-pendulum-like phenomenon. This part will be discussed in next section.

## 1.2. Inverse Pendulum Control

In this section of the report, inverse pendulum phase of the wheelchair in hand is discussed. In figure 1, step climbing system stages are shown. Both cases of human assisting and robotic assisting is presented in the figure. As it is obvious, this report will investigate the control at the stage of Inverse Pendulum phase.

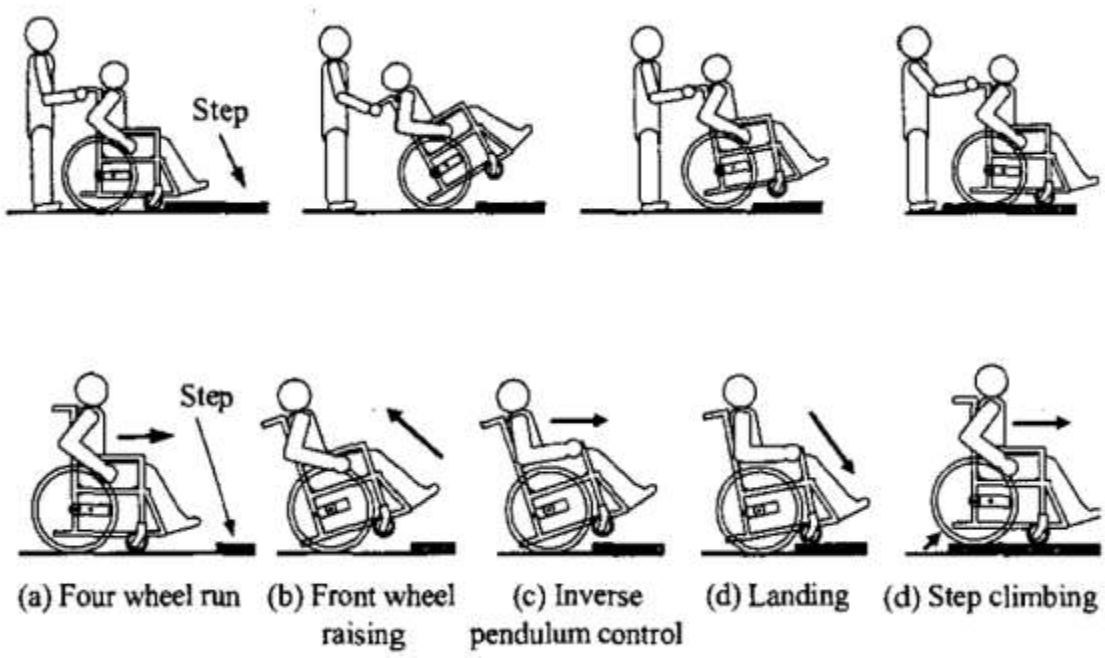


**Figure 1: Step Climbing Stages**

As shown in figure 1(c), the robotic assist wheelchair will impose a balancing mechanism to help the person onboard. The original project mechanism will be explained in next section.

## 1.3. Wheelchair Mechanism

In this section, the hardware mechanism proposed is to be discussed. The balancing mechanism is established by controlling the rear wheel rotation. Rear wheel drive system consists of DC motor, gearbox, chain and housing. The gear ratio is 772 making a reduction ration of 1/772.

Two sensors are implemented to give the required measurements. An optical encoder is mounted to detect the rotation of the rear wheel. A gyro sensor is put to measure the rate of inclination of the wheelchair body. The 'control' system consists of a personal computer, counter board, Analog-to-Digital converter and Digital-to-Analog converter. Figure 2 shows a schematic of the hardware system of the wheelchair.

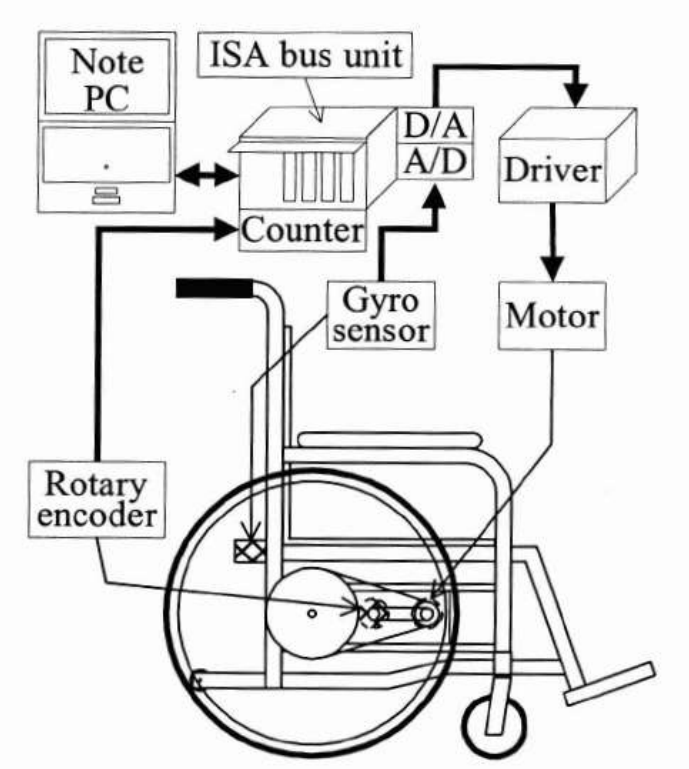


**Figure 2: Hardware System of the Wheelchair**

The mechanism goes as follows:

1) Gyro sensor detects the inclination velocity the wheelchair

2) Inclination velocity is put into the PC through Analog-to-Digital converter
3) Inclination velocity is subtracted by a bias signal measured previously
4) Inclination velocity is integrated to give the inclination angle of the wheelchair
5) The error is computed by subtracting the desired value from the measure inclination
6) The error signal is put into the controller
7) A control input is produced and using Digital-to-Analog converter to send the current required to drive the DC motor… and so

The sampling period used in the original work was 17 ms.

# 2. Dynamic Model Development

In this big part of the report, a thorough discussion of the dynamic model of the wheelchair in inverse pendulum phase is established. Brief remarks about the dynamics of a general inverse pendulum system are explained. Then, the overall wheelchair dynamics is discussed. The mathematical model of the system is then discussed also. The State-Space model is then discussed in details. Discussion of the properties of the real system used in experiment are finally concluding this section of the report

## 2.1. Inverse Pendulum Dynamics

It is well known that Inverse Pendulum is a significant system that used widely in control research and applications especially in Academia. This system is investigated heavily because of its relation to other control theory studies of missile guidance, self-balancing transportation systems (as the system in hand) and lifting cranes.

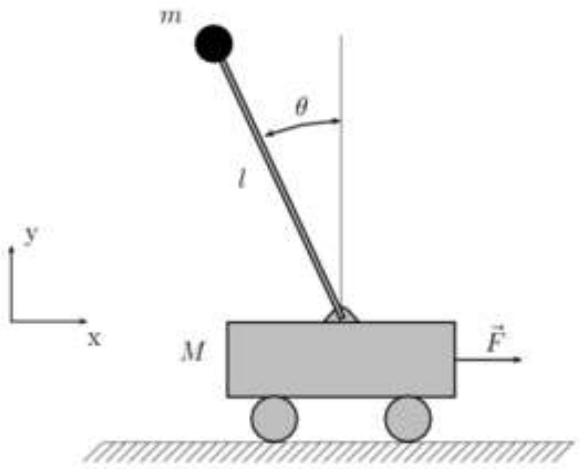


**Figure 3: Schematic of an Inverse Pendulum on a Cart**

An inverse pendulum system is known to be nonlinear. As shown in figure 3, an inverse pendulum on a cart is viewed. Obtaining the equation of motion of the system is done via the derivations from Lagrange's Equations of motion. Originally, two differential equations describe the motion of inverse pendulum system.

$$(M+m)\ddot{x} + ml\ddot{\theta}\cos\theta - ml\dot{\theta}^2\sin\theta = F$$

$$ml\left(-g\sin\theta + \ddot{x}\cos\theta + l\ddot{\theta}\right) = 0$$

As '*M*', represents mass of the cart, '*m*', being the mass of pendulum point, '*x*' being the translational position of the system, '*l*', representing length of the pendulum, '*F*' is the input force and '$\theta$' is the angle of the pendulum with

respect to the vertical direction. As it is obvious the nonlinearity is on '$\theta$' from the existence of *sine* and *cosine* functions.

## 2.2. Wheelchair Dynamics

In this section, the overall wheelchair dynamics is discussed. Of course, wheelchair dynamics in hand is investigated during the inverse pendulum stage. Figure 4 shows an overview picture of the wheelchair dynamic model.

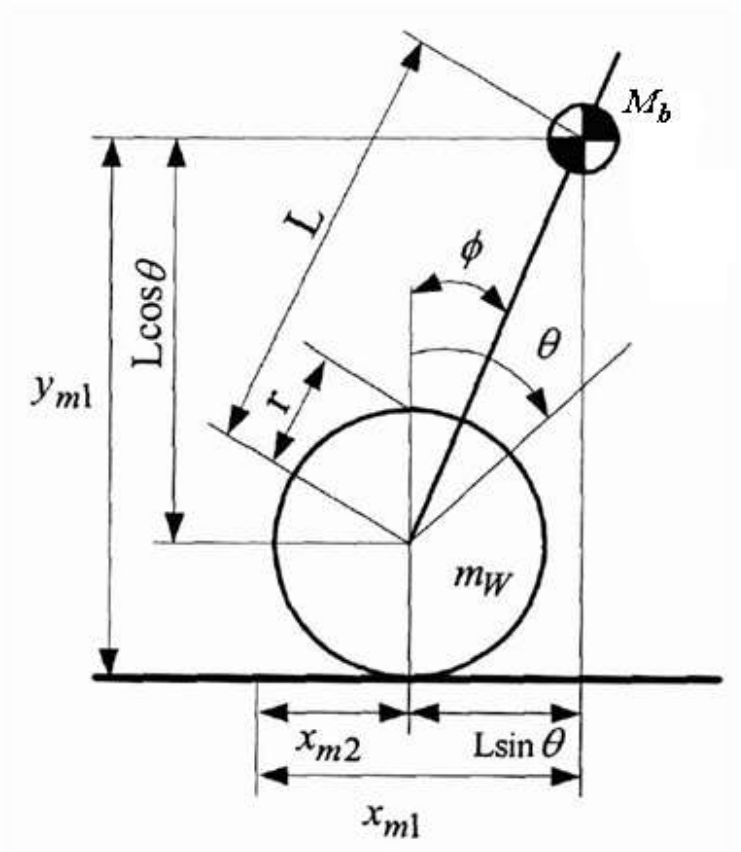


**Figure 4: Wheelchair Dynamics**

This model in figure 4 can be projected to figure 3 of the inverse pendulum on a cart. As $M_b$ in figure 4 being the center-of-mass mass of the wheelchair body is projected as the point mass of the pendulum. And $\phi$ is the inclination angle of the pendulum. The translational motion of 'x' in figure 3 is here in figure 4 done through the rotation of the rear wheel represented here by $\theta$. And r and $M_w$ represent radius of the rear wheel and mass of rear wheels respectively. It is assumed that the two rear wheels act as a one with no consideration of each wheel dynamics. So the 'only' impact of the wheelchair on an inverse pendulum system is that the translational motion is now coming from the motor-controlled rear wheel rotation.

The result of the above discussion is to form the complete equations of motion of the wheelchair nonlinear dynamic system. The two differential equations describing the motion is

$$\left(M_b L^2 + J_b + J_m K_g^2\right)\ddot{\phi} + \left(M_b rL\cos\phi - J_m K_g^2\right)\ddot{\theta} + K_{cs}\left(\dot{\phi} - \dot{\theta}\right)$$

$$- M_b gL\sin\phi = -\frac{K_g K_t}{R} v \qquad \ldots \quad (1)$$

$$\left(M_b rL\cos\phi - J_m K_g^2\right)\ddot{\phi} + \left[(M_b + M_w)r^2 + J_w + J_m K_g^2\right]\ddot{\theta} - K_{cs}\dot{\phi}$$

$$+ \left(K_{cs} + K_{cf}\right)\dot{\theta} - M_b rL\sin\phi \cdot \dot{\phi}^2 = \frac{K_g K_t}{R} v \qquad \ldots \quad (2)$$

The parameters and variables involved in the equations, and will be used throughout the whole report, are defined as

**Table 1: Wheelchair Parameters & Variables**

| |
|---|
| $\phi \rightarrow$ Inclination angle of the wheelchair body [rad] |
| $\theta \rightarrow$ Rotation angle of the rear wheels [rad] |
| $v \rightarrow$ Input voltage of the DC motor [V] |
| $R \rightarrow$ DC motor resistance [ohm] |
| $M_b \rightarrow$ Total mass of the wheelchair body and person onboard [kg] |
| $M_w \rightarrow$ Mass of the rear wheels [kg] |
| $J_b \rightarrow$ Total moment of inertia of the wheelchair body and person [kg.m$^2$] |
| $J_w \rightarrow$ Moment of inertia of the rear wheels [kg.m$^2$] |
| $L \rightarrow$ Length between wheelchair shaft & gravity center of wheelchair body [m] |
| $r \rightarrow$ Radius of the rear wheels [m] |
| $K_{cf} \rightarrow$ Damping constant between floor and rear wheels [N.m/(rad/s)] |
| $K_{cs} \rightarrow$ Damping constant of the wheel shaft [N.m/(rad/s)] |
| $K_t \rightarrow$ Torque constant of the DC motor [N.m/A] |
| $K_g \rightarrow$ Gear ratio |

## 2.3. Linearized Mathematical Model

In this section, only the linearization process is done on the dynamic model to have it ready for analysis and design.

As the goal is to have the inclination angle close to zero, the linearization goes by using these properties:

$$\sin\phi \approx \phi$$

$$\cos\phi \approx 1$$

$$\dot{\phi}^2 \approx 0$$

So, by that, the final linearized mathematical model is

$$\left(M_b L^2 + J_b + J_m K_g^2\right)\ddot{\phi} + \left(M_b rL - J_m K_g^2\right)\ddot{\theta} + K_{cs}\left(\dot{\phi} - \dot{\theta}\right) - M_b gL\phi = -\frac{K_g K_t}{R} v \quad \ldots (3)$$

$$\left(M_b rL - J_m K_g^2\right)\ddot{\phi} + \left[(M_b + M_w)r^2 + J_w + J_m K_g^2\right]\ddot{\theta} - K_{cs}\dot{\phi} + \left(K_{cs} + K_{cf}\right)\dot{\theta} = \frac{K_g K_t}{R} v \quad \ldots (4)$$

## 2.4. State-Space Model

This section is will present the complete state-space model of the system. From the linearized equations of motion of (3) and (4) in previous section, the complete State-Space Model of the Robotic Wheelchair during Inverse Pendulum Control is

$$\dot{x} = Ax + Bu$$

$$y = Cx$$

With the state vector of,

$$x = \begin{bmatrix} \phi \\ \theta \\ \dot{\phi} \\ \dot{\theta} \end{bmatrix}$$

With,

$$A = \begin{bmatrix} 0 & 0 & 1 & 0 \\ 0 & 0 & 1 & 0 \\ A_1 & 0 & -A_2 & A_3 \\ -A_4 & 0 & A_5 & -A_6 \end{bmatrix} \quad , \quad B = \begin{bmatrix} 0 \\ 0 \\ -B_1 \\ B_2 \end{bmatrix}$$

As,

$$A_1 = \frac{a_4 b_1}{a_1 b_1 - a_2^2} \quad , \quad A_2 = \frac{a_2 a_3 + a_3 b_1}{a_1 b_1 - a_2^2} \quad ,$$

$$A_3 = \frac{a_2 b_2 + a_3 b_1}{a_1 b_1 - a_2^2} \quad , \quad A_4 = \frac{a_2 a_4}{a_1 b_1 - a_2^2} \quad ,$$

$$A_5 = \frac{a_2 a_3 + a_1 a_3}{a_1 b_1 - a_2^2} \quad , A_6 = \frac{a_2 a_3 + a_1 b_2}{a_1 b_1 - a_2^2} \quad ,$$

$$B_1 = \frac{a_2 a_5 + a_5 b_1}{a_1 b_1 - a_2^2} \quad , B_2 = \frac{a_2 a_5 + a_1 a_5}{a_1 b_1 - a_2^2} \quad ,$$

With,

$$a_1 = M_b L^2 + J_b + J_m K_g^2 \quad , \quad a_2 = M_b r L - J_m K_g^2$$

$$a_3 = K_{cs} \quad , \quad a_4 = M_b g L \quad , \quad a_5 = \frac{K_g K_t}{R}$$

$$b_1 = (M_b + M_w) r^2 + J_w + J_m K_g^2 \quad , \quad b_2 = K_{cs} + K_{cf}$$

*Remark: in (Takahashi, et al., 2000) paper, the authors made a typing error (typo) for the value of* $A_5$ *as first* $a_3$ *in the numerator is miss-typed as* $b_3$.

Putting in mind that the measured outputs are optical encoder output $(\phi - \theta)$ and the output of the gyro sensor $\dot{\phi}$. So, this makes

$$C = \begin{bmatrix} 1 & -1 & 0 & 0 \\ 0 & 0 & 1 & 0 \end{bmatrix}$$

And system input $u = v$ the DC motor input voltage

## 2.5. System Configuration & Test Simulations

In this brief section, just values of parameters of the system will be presented and some simulations to give an overview picture about the situation in hand.

Parameters values of the system that will be used throughout the system is presented in the following table 2.

**Table 2: System Parameters Values**

| | |
|---|---|
| $R$ | 0.84 [ohm] |
| $M_w$ | 6.52 [kg] |
| $L$ | 0.29 [m] |
| $K_t$ | 0.0239 [N.m/A] |
| $J_w$ | 0.11 [kg.m$^2$] |
| $K_{cf}$ | 8.78 [N.m/(rad/sec)] |
| $K_{cs}$ | 12.3 [N.m/(rad/sec)] |
| $M_b$ | 84.16 [kg] |
| $J_b$ | 29.3 [kg.m$^2$] |
| $r$ | 0.305 [m] |
| $K_g$ | 772 |

| | |
|---|---|
| $J_m$ | $7.0\text{x}10^{-6}$ [kg.m$^2$] |

So, because no control is yet designed, performing an uncontrolled-system simulation is done here. Here and throughout the whole report, all computer simulations and codes are done under **MATLAB R2007b** environment.

So, the numeric full state-space model is

$$\dot{x} = \begin{bmatrix} 0 & 0 & 1 & 0 \\ 0 & 0 & 0 & 1 \\ 6.0236 & 0 & -0.3895 & 0.4464 \\ -1.5498 & 0 & 1.0674 & -1.7724 \end{bmatrix} x + \begin{bmatrix} 0 \\ 0 \\ -0.6955 \\ 1.9061 \end{bmatrix} u$$

$$y = \begin{bmatrix} 1 & -1 & 0 & 0 \\ 0 & 0 & 1 & 0 \end{bmatrix} x$$

So using an initial condition of

$$x(0) = \begin{bmatrix} -12° \\ 0 \\ 0 \\ 0 \end{bmatrix} = \begin{bmatrix} -0.21 \\ 0 \\ 0 \\ 0 \end{bmatrix} (rad)$$

So a test simulation of the autonomous system:

$$\dot{x} = Ax$$

is showed in figure 5.

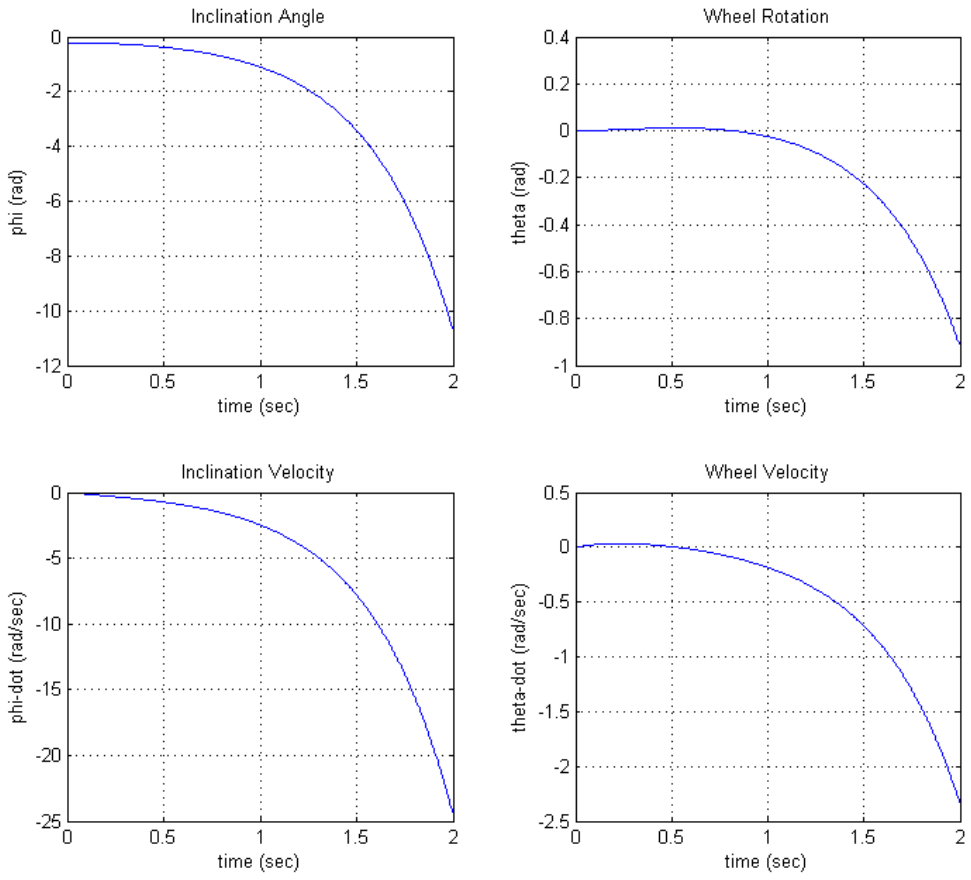


**Figure 5: State Simulation Results for uncontrolled system**

This behavior of the states is expected. The system is obvious to be unstable. The conclusion is coming from the nature of the mechanical system involved. It is expected for the machine to lose balance very fast. And by scientific means, the autonomous system is found to be unstable due to the eigenvalues of the system are

0, 2.2871, -2.9879 & -1.4611

with two nonnegative eigenvalues appearing.

# 3. Optimal Control Design & Results

This would be the main part of the report. This section will discuss in detail different control designs. The different control strategies that will be discussed here include:

1) Linear Quadratic Regulator (LQR) design
2) Linear Quadratic Gaussian Regulator (LQG) design
3) $H_2$ Control design
4) $H_\infty$ Control design

Every design will be discussed in detail in using the Robotic Wheelchair state-space model which explained in earlier sections of the report. Each design will be presented along with all the simulation results and comments about the results produced.

## 3.1. Linear Quadratic Regulator (LQR) Design

In this section, the LQR design approach will be used. Before continuing with the control design, some assumptions must be set. Here, we assume the full

availability of the states of the system to have them fed back to the controller, which is not the case. The only available physical outputs of the system are the gyro sensor output and the encoder output. Of course the straightforward assumption is that the LQR design does not include any external disturbances affecting the states of the system.

Establishing the LQR cost function of,

$$J = \int_0^\infty x^T Q x + u^T R u \, dt$$

$$s.t. \quad \dot{x} = Ax + Bu$$

With (as defined in earlier sections of the report),

$$A = \begin{bmatrix} 0 & 0 & 1 & 0 \\ 0 & 0 & 0 & 1 \\ 6.0236 & 0 & -0.3895 & 0.4464 \\ -1.5498 & 0 & 1.0674 & -1.7724 \end{bmatrix} \quad \& \quad B = \begin{bmatrix} 0 \\ 0 \\ -0.6955 \\ 1.9061 \end{bmatrix}$$

The optimal designs established are obtained by setting different weights on the states and input.

*Note: all MATLAB codes can be found in Appendix or the included CD.*

- **The first case** is with putting unity weights on the states and the input. The results obtained are shown in figure 6.

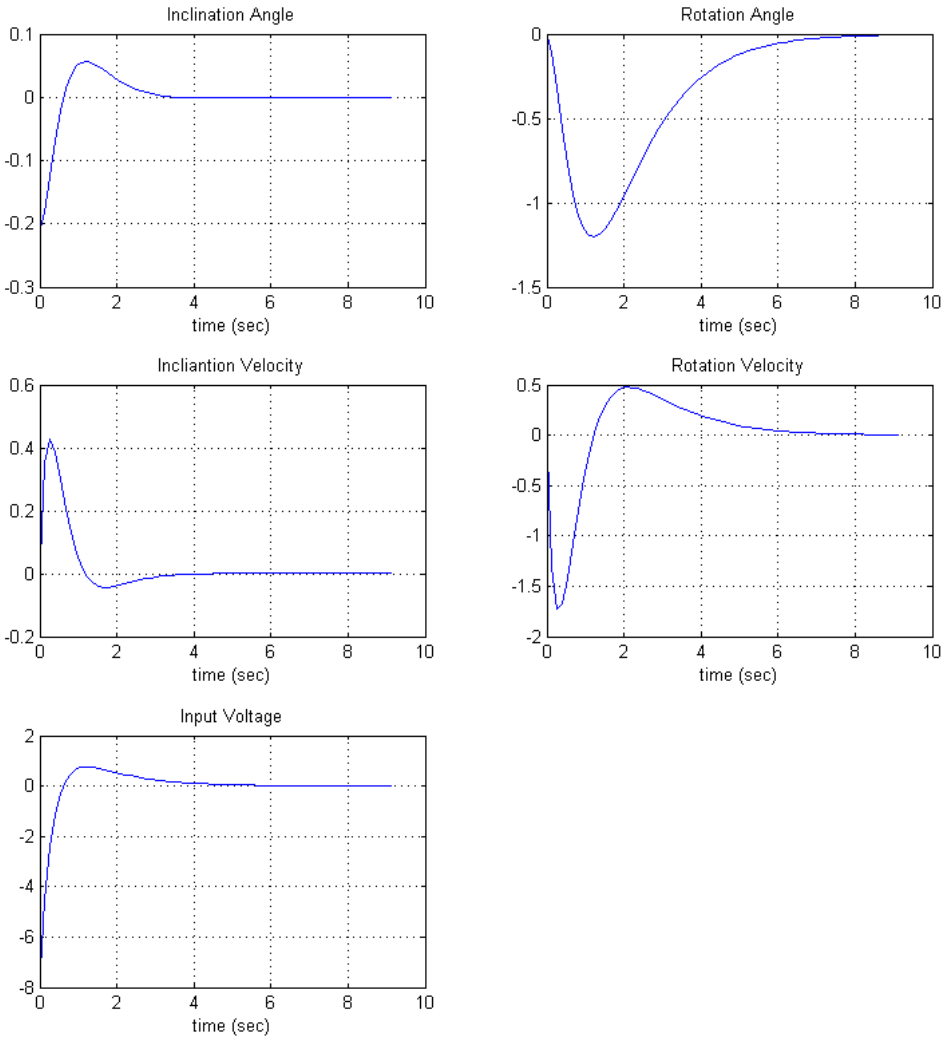


**Figure 6: LQR case 1 results**

This trivial design gives us fancy results. As our goal is to control and regulate the inclination of the wheelchair, the settling time found to be relatively acceptable (~3 sec). An overshoot is observed in all states and input.

- **Another case** is to put only weight on inclination angle or only on wheel rotation. Both cases are shown in figure 7.

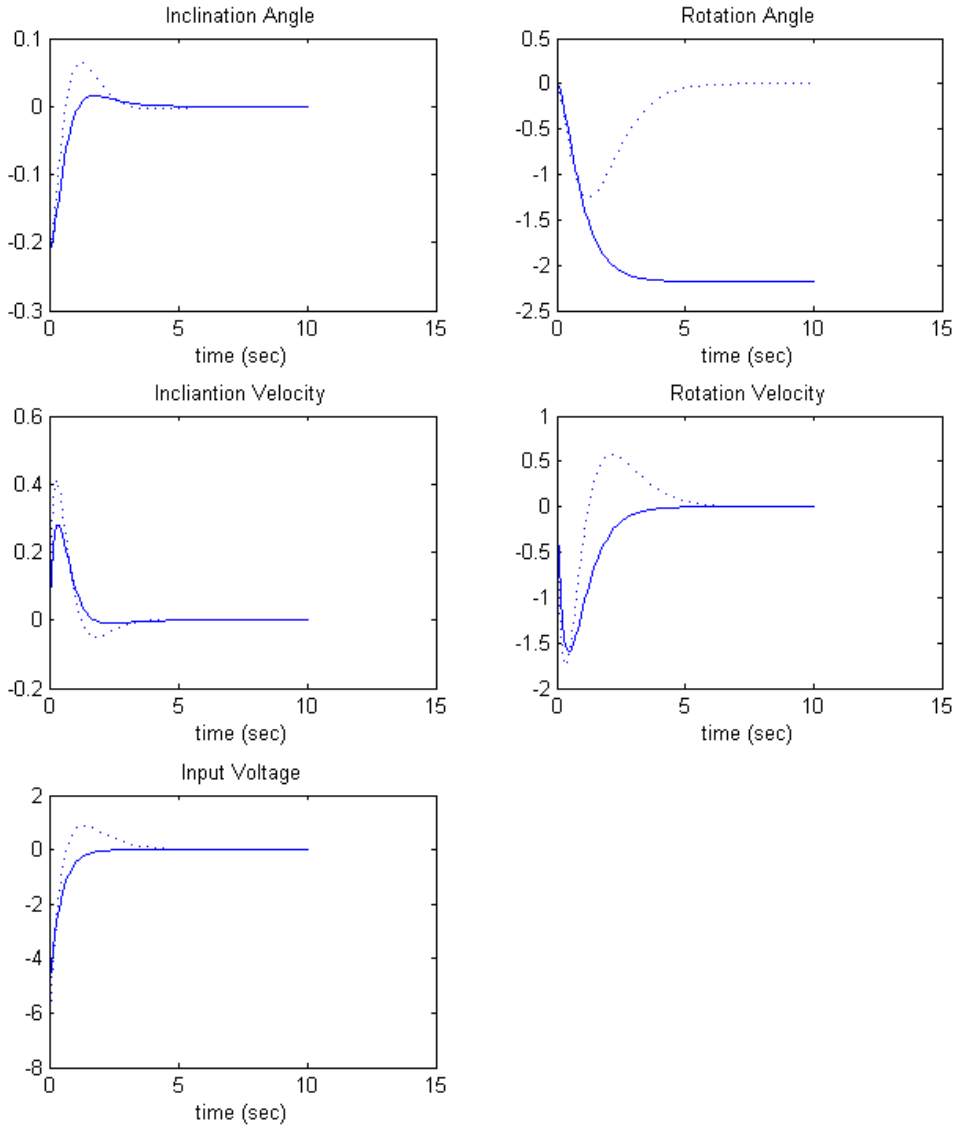


**Figure 7: LQR weight on 'phi' or on 'theta'**

In figure 7, The solid line corresponds to unit weight on the inclination only. The light (dotted) line corresponds to a unit weight on wheel rotation only. Interestingly, sole weight on the inclination angle made a better performance.

This is expected because wheels behavior left freely. There are almost no overshoot on input and inclination in the case with weight only on inclination.

- Another case of LQR is just to put weights on both inclination and wheel rotation and observe change when increasing. The result is depicted in figure 8.

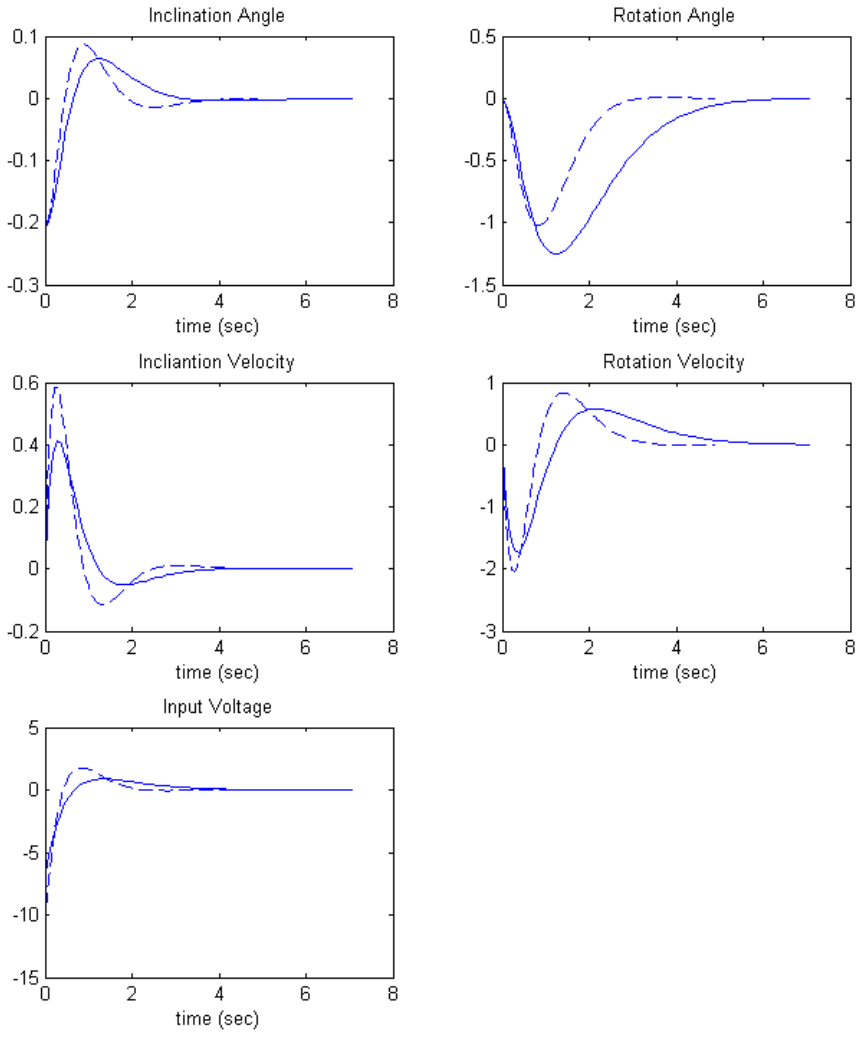


**Figure 8: LQR weights on both inclination & wheel rotation**

In figure 8, the solid line corresponds to a unit weight on both inclination angle and wheel rotation. Dashed line corresponds to an increase in weight on both by 10. Decrease in settling time is viewed by increasing the weight, but with increase in the overshoots of the states. Of course slight increase on overshoot of the input is resulted after increasing the weight.

## 3.2. Linear Quadratic Gaussian Regulator (LQG) Design

In this section, the more practical design strategy is used. Linear Quadratic Gaussian Regulator (LQG) method depends on the state estimation through the information of the input and output of the system. This estimation and regulation is also used to eliminate the effects of noise or external disturbances on the states of the problem.

As the system is expected to receive noise, the state-space model here is going to be modified to introduce the noise input along with the original input. So, the state-space model will be formed as

$$\dot{x} = Ax + Bu + B_w w$$

As '*w*' represents the external noise to the states.

Analyzing the system of the robotic wheelchair and state variables, the value of $B_w$ is left to be investigated. The value will express how noise input will affect the states. Considering the overall mechanical system of the robotic wheelchair in inverse pendulum stage, largest effect of the noise will be on the inclination (balance) of the system. A slight smaller effect is translated into the inclination velocity from noise to the gyro sensor. But much smaller disturbance would be observed on both wheel rotation and wheel velocity states.

So, a predicted values can be used are

$$B_w = \begin{bmatrix} 0.09 \\ 0.025 \\ 0.075 \\ 0.05 \end{bmatrix}$$

Values are chosen to be somehow small because of expecting a unit noise input will affect the states which are having the small units of radians.

Before showing the results of the different designs of LQG, a brief explanation of how the control procedure will go. State estimation is required because the lack of full state measuring. The only available are the output. State estimation is done through an observer system. A usual and well renowned estimation method is the **Kalman Filtering**.

Basically, the State-Estimator or the Kalman Filter is of the form of

$$\dot{x}_e = Ax_e + Bu + L(y - Cx_e)$$

$$\begin{bmatrix} y_e \\ x_e \end{bmatrix} = \begin{bmatrix} C \\ I \end{bmatrix} x_e$$

With $x_e$ corresponds to the estimated states. And $L$ is the estimator gain calculated. For the specific system in hand, using a unity noise covariance, the state estimator system is

$$\dot{x}_e = \begin{bmatrix} -0.6822 & 0.6822 & -0.7367 & 0 \\ -0.05607 & 0.05607 & -0.178 & 1 \\ 4.465 & 1.559 & -4.358 & 0.4464 \\ -1.7 & 0.15 & 0.6861 & -1.772 \end{bmatrix} x_e + \begin{bmatrix} 0 & 0.6822 & 1.737 \\ 0 & 0.05607 & 0.178 \\ -0.6955 & 1.559 & 3.968 \\ 1.906 & 0.15 & 0.3813 \end{bmatrix} \begin{bmatrix} v \\ \theta - \phi \\ \dot{\phi} \end{bmatrix}$$

As it is obvious, estimator inputs are the system input, optical encoder output and gyro sensor output.

By the separation principle, an independent computation of the feedback control gain is done using the information of the original system before estimation. Several cases are tested using LQG design. Different weights on states and input are tested and investigated.

- **The trivial case** is to try the unity weights on the states and input.

The result of this design can be viewed in figure 9.

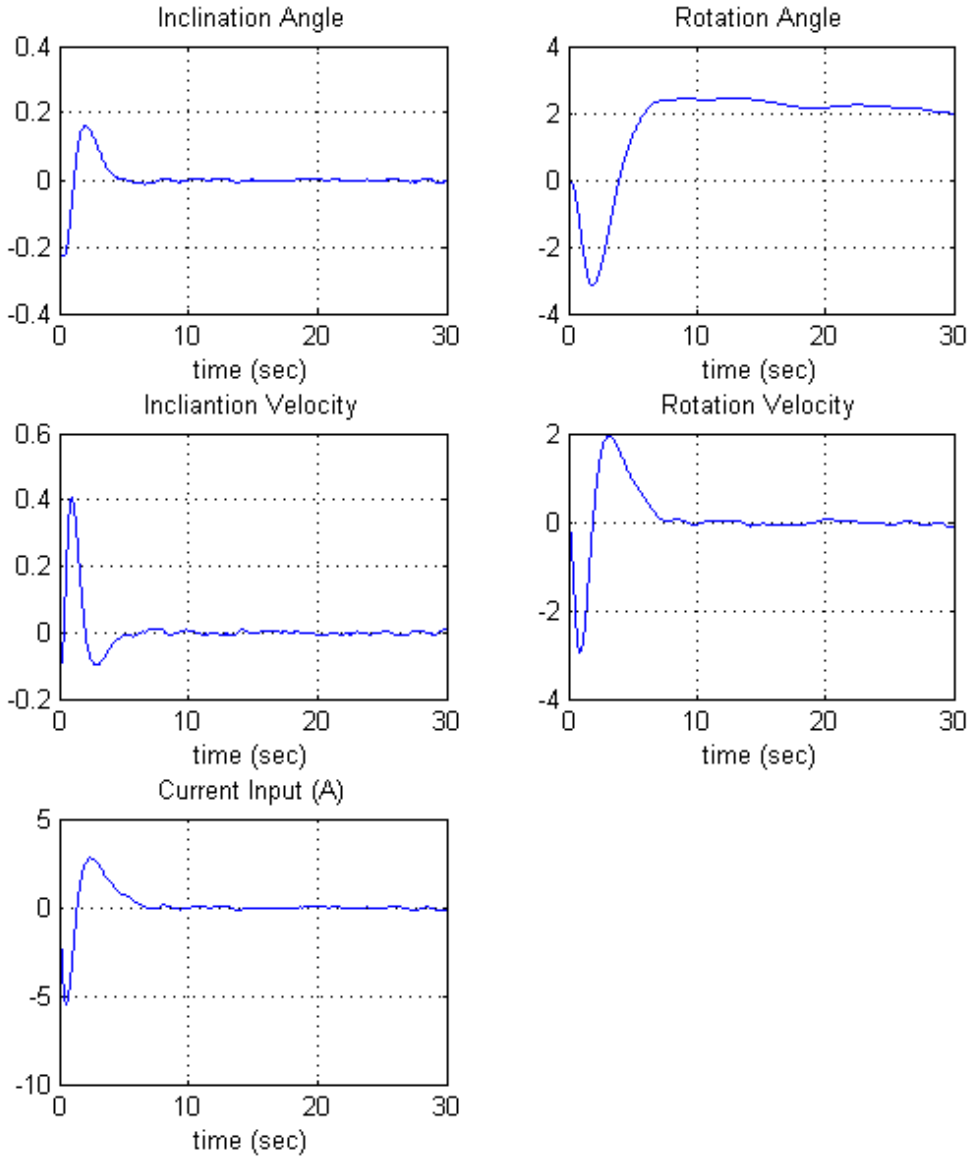


**Figure 9: LQG with unity weights**

The main observation is the relatively high settling time. This is expected due to the introduction of the estimator system. It is observed that wheel rotation

takes very long time to reach zero. A relatively unwanted overshoots are observed, specially the overshoot of the inclination.

- **Another case** is to put unity weights on only the inclination or only on the wheel rotation.

The result of this is shown in figure 10.

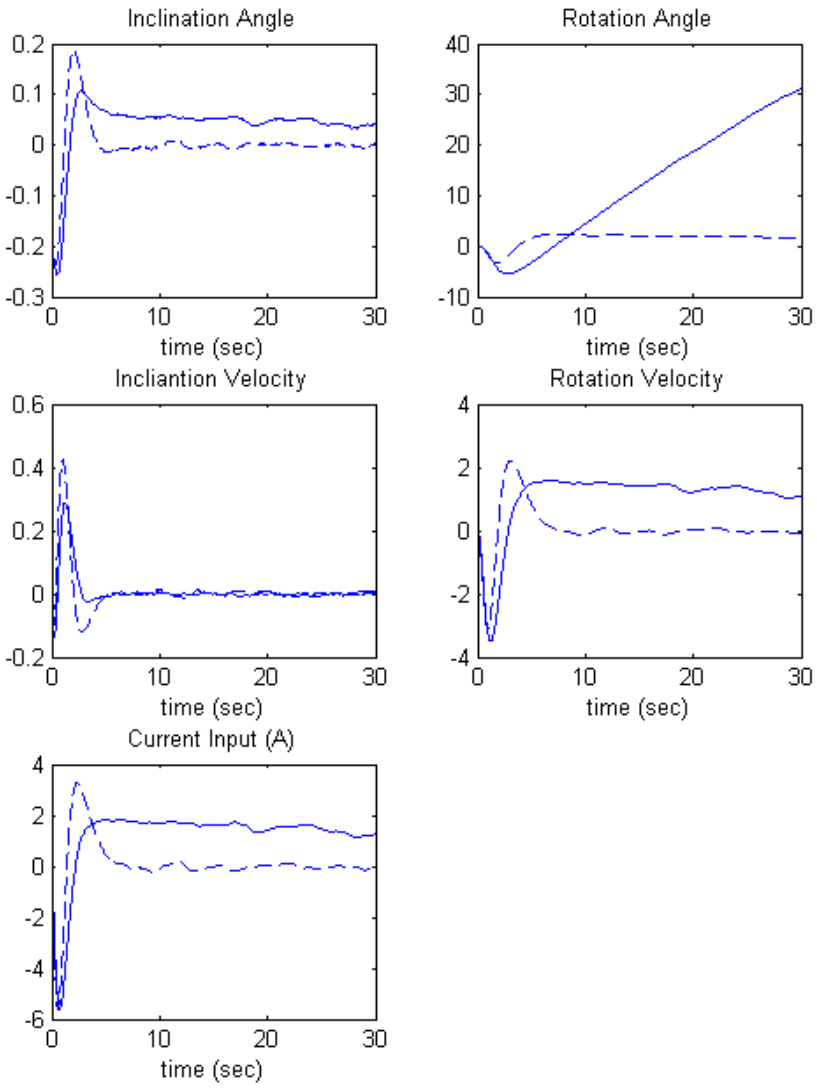


**Figure 10: LQG 2nd case**

It is clearly obvious that big difference between the two cases. The solid line corresponds to weight on inclination. The dashed line corresponds to weight on wheel rotation. When having weight on inclination only, settling time increases, but overshoots are 'significantly' decreased. Faster response is found by the weight on the wheel rotation. But in general, both performances are better than putting unity weights on all states as compared to figure 9.

- **Another case** is to put weight on both states.

Actually, there is no need to put the result because it is almost the same as the performance attained by putting unity weights on all states as in figure 9.

- **Another case** is to observe the change of weight on the control input.

The design is obtained by putting 0.1 and 10 as weights on the control input. The result is shown in figure 11.

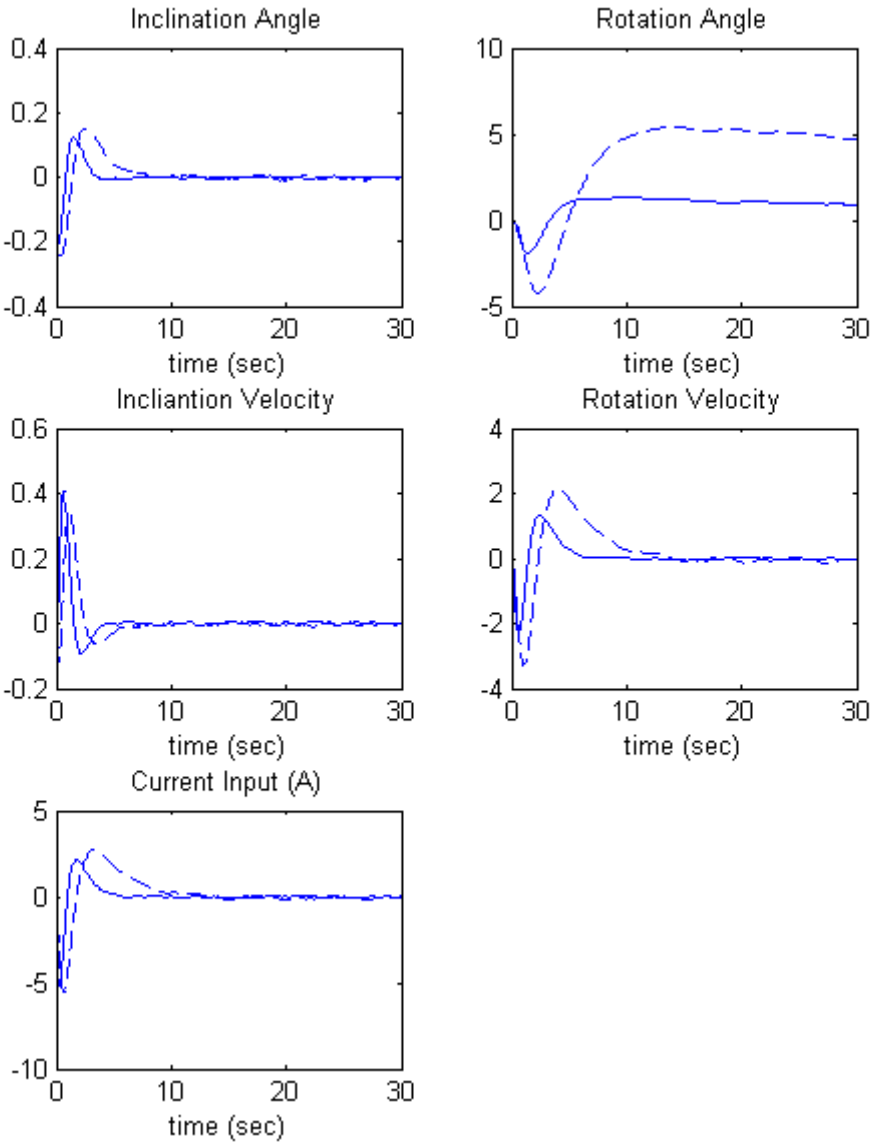


**Figure 11: LQG different weights on input**

Strangely, putting less weight of 0.1 (solid) on the input gives the 'relative' better performance than larger weight of 10 (dashed). Big difference is observed on wheel rotation. Control input almost not changed. But in general, putting more weight on input gives slower response.

## 3.3. $H_2$ Control

In this part, the $H_2$ norm is to be minimized through the approach of Linear Matrix Inequalities (LMI). With no constraints on input or states, the result of the minimizing problem is shown in figure 12.

An evaluation output is set to be $z = [1 \quad 0 \quad 0 \quad 0]x$

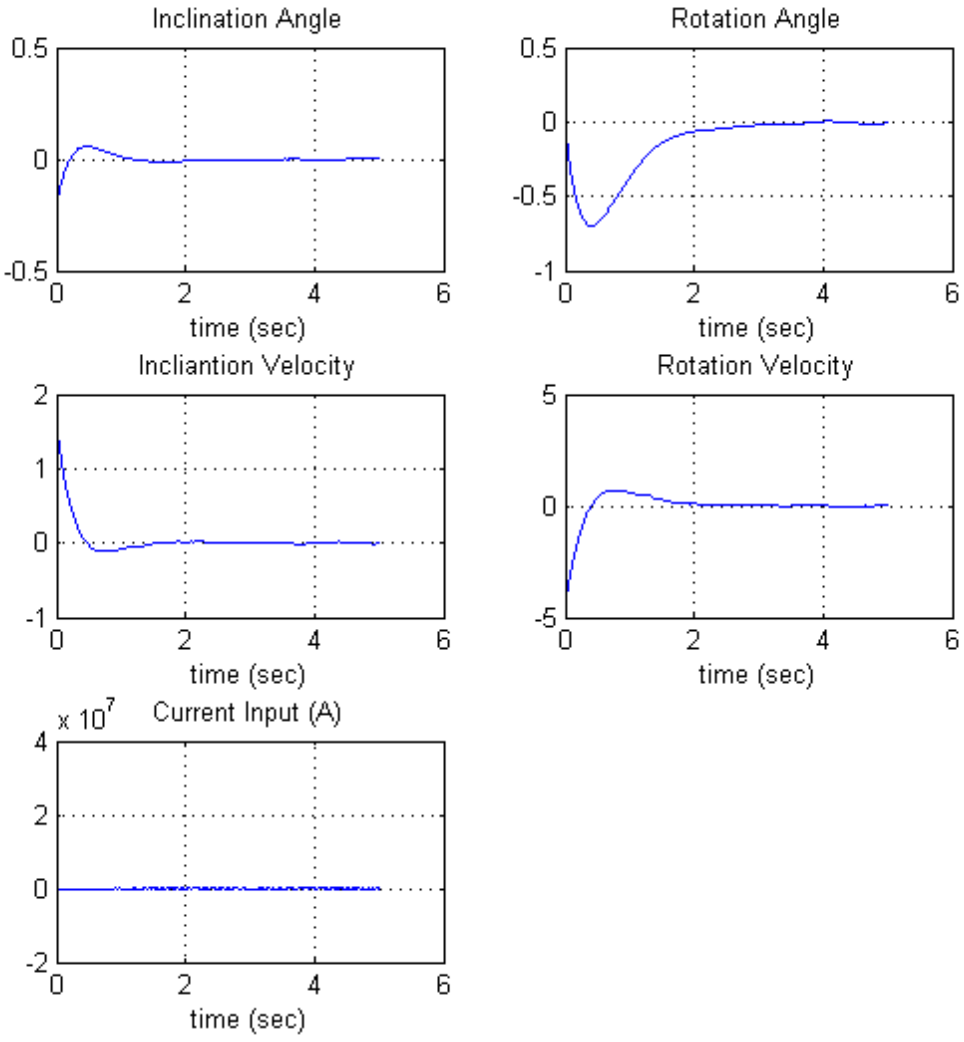


**Figure 12: H2 control**

The minimizing problem gives extraordinarily results. You can not accept the four states performance with the too huge impulse effect of the input. H2 control proved that at least for this system is so not practical. The minimum H2 norm value found is 0.5077.

The problem changed to have a constraint on the minimization of the H2 norm. However, almost identical results are produced as in figure 12.

## 3.4. $H_\infty$ Control

In this part of the report, the $H_\infty$ norm is minimized. The minimization is done by the LMI approach. Having no constraints on the minimization, the result of the minimization gives also unpractical values like H2 problem. The result of the minimization gives a optimal $H_\infty$ norm value of 0.018.

But different than H2 problem, putting constraint on the minimization of

$$\|\cdot\|_\infty < \gamma$$

With $\gamma = 0.5$ gives a result as shown in figure 13.

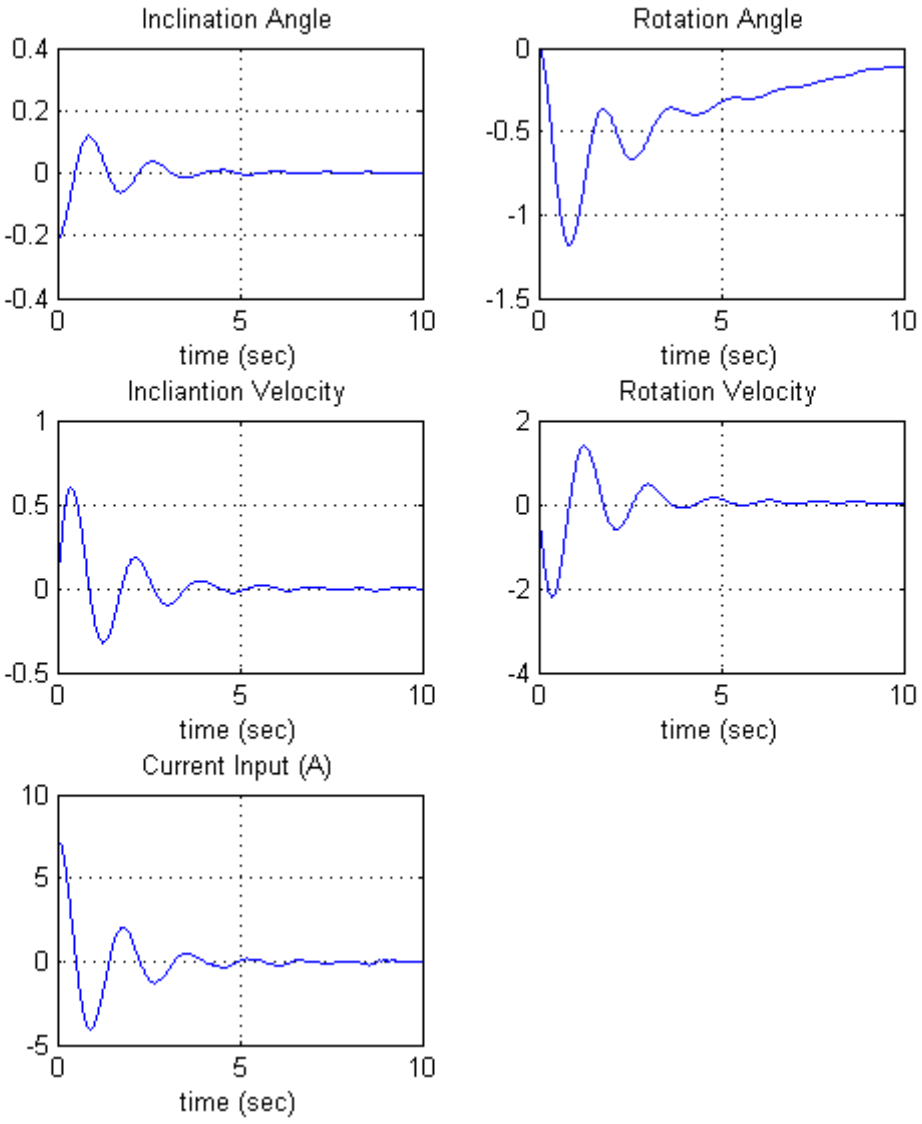


**Figure 13: H-infinity Control**

This minimization problem introduces an oscillatory behavior on the states. Relatively high input values are resulting also.

## 3.5. LQR with Integral Action

In this part, an integral action is added to the original LQR design.

So, with,

$$A_w = \begin{bmatrix} A & \vdots & 0 \\ \cdots & & \cdots \\ C & \vdots & 0 \end{bmatrix}, \qquad B_w = \begin{bmatrix} B \\ \cdots \\ 0 \end{bmatrix}$$

$$Q = \begin{bmatrix} C^T C & \vdots & 0 \\ \cdots & & \cdots \\ 0 & \vdots & \sigma I \end{bmatrix}, R = \rho I$$

With $\rho = 0.01$ and $\sigma = 1$

The result of the control is shown in figure 14.

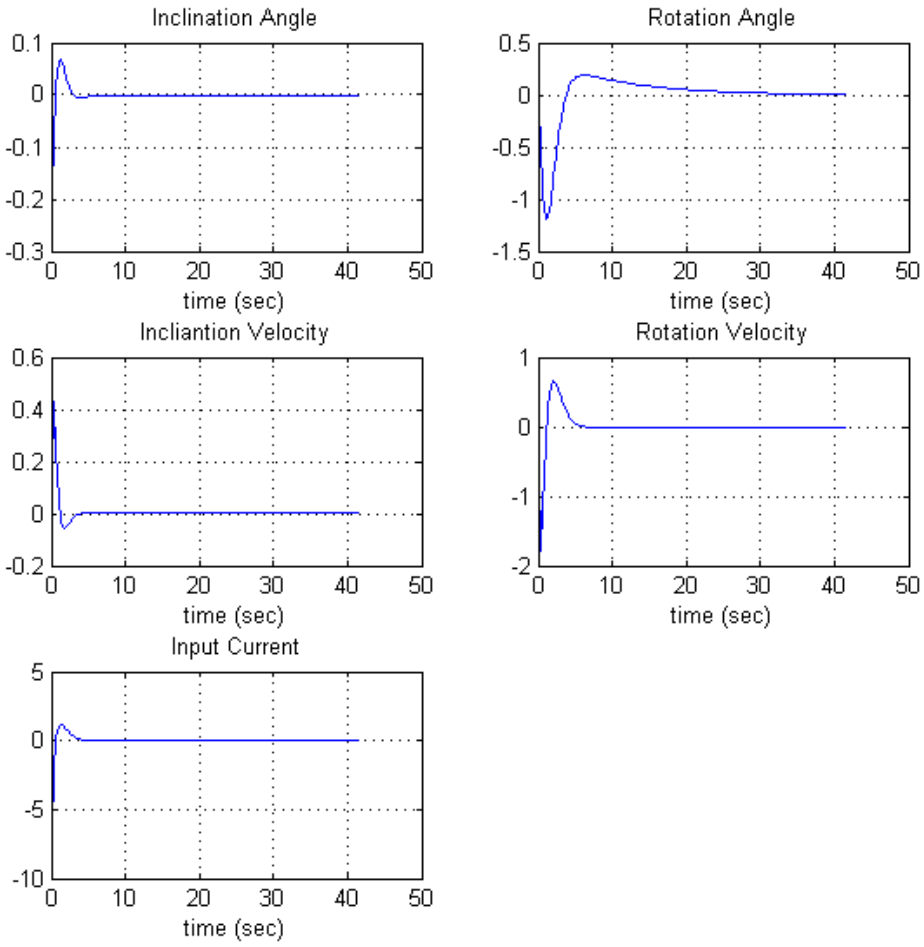


**Figure 14: LQR with Integral Action**

The integral action improved the overshoot problem significantly. Slightly big initial input is observed also.

## 3.6. Control Design Robustness

This very small part is only to observe the robustness of the control designs obtained. Here, only the case of LQG will be tested with changes in model

parameters. The same design (i.e. same feedback gains and estimation) of the LQG design obtained with unity weights on all states and input.

First case with increase in rear wheel radius of 25% is shown in figure 15.

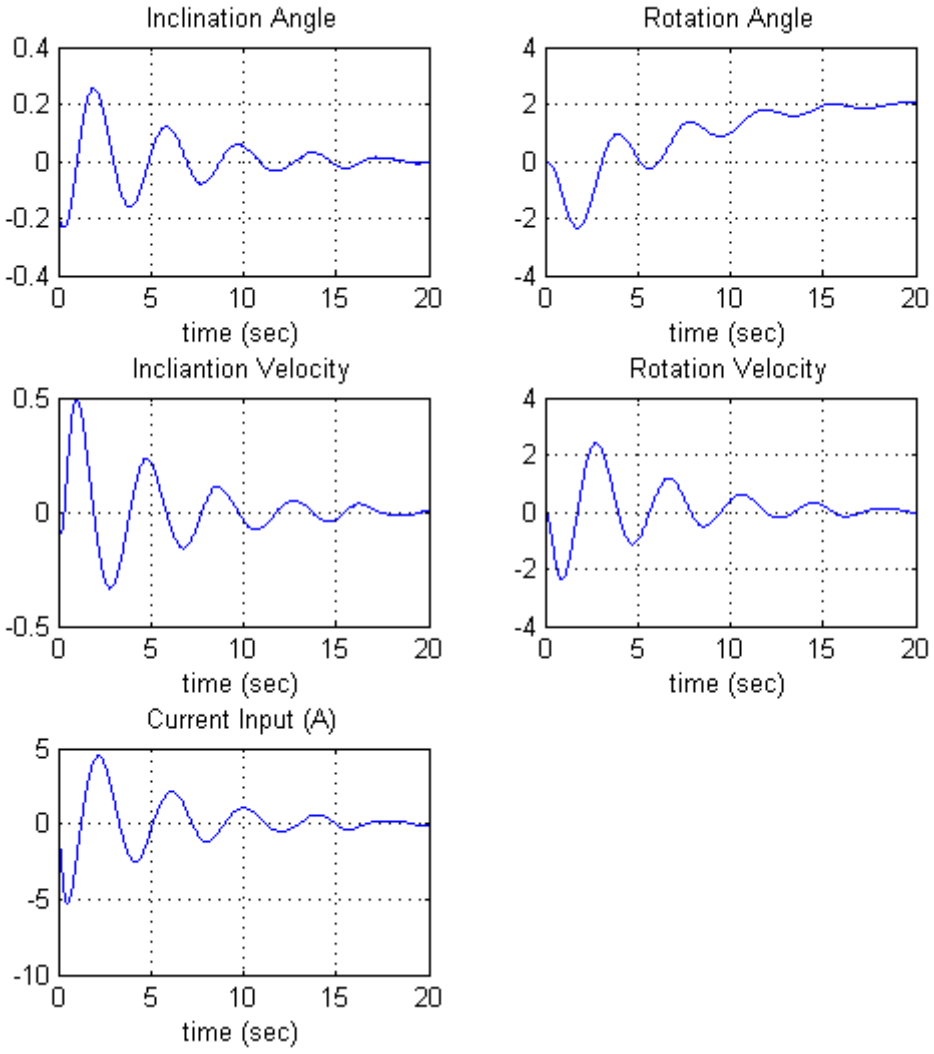


**Figure 15: LQG with change in wheel radius**

Another more logical uncertainty can be coming from the person onboard changing the mass, changing the inertia or change in the distance between the center of mass and the wheel shaft. So, in figure 16, an increase of 25% is put onto the distance, total mass and total moment of inertia.

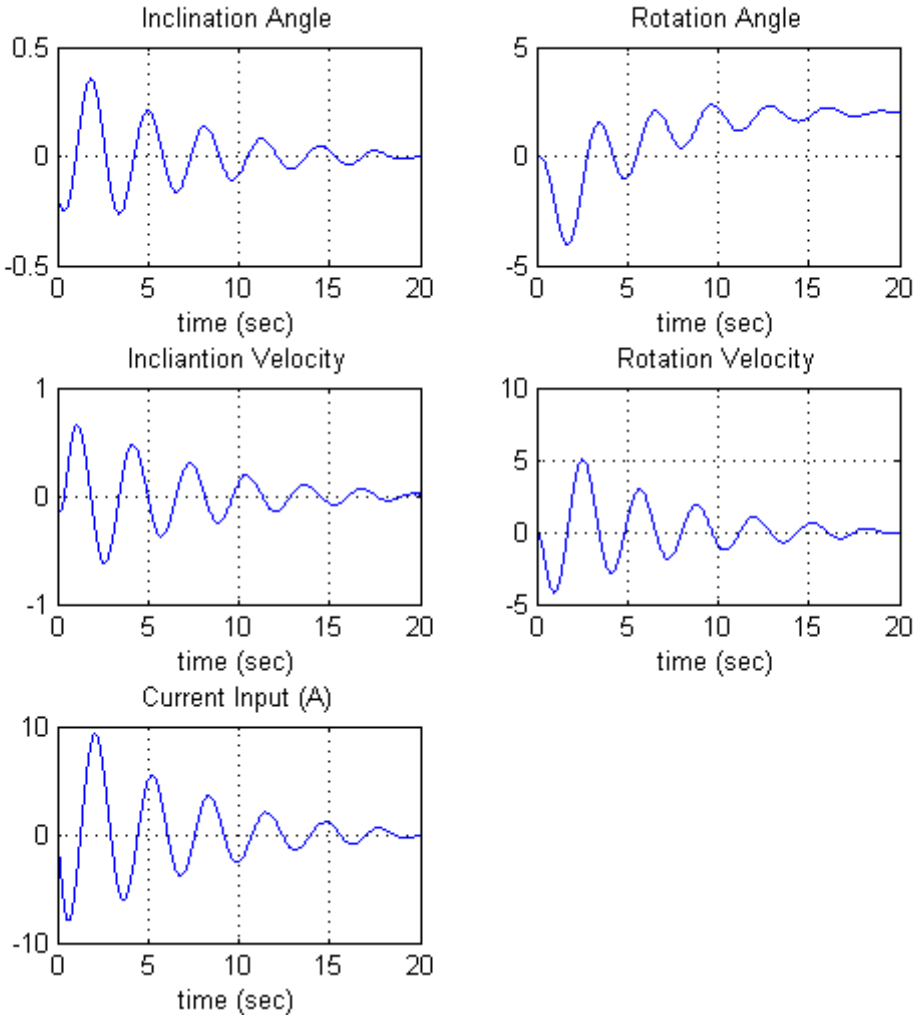


**Figure 16: LQG with different uncertainties**

The design can be evaluated according to these results as relative good because of the introduction of oscillations. But as long as stability is maintained, the design is acceptable.

# 4. Conclusion & Future Improvements

This is the final section of the report. It is observed from the thorough study established in this report that Optimal Control design gives powerful tool to control real-life applications.

From the designs investigated throughout the report, LQG appeared to be the best design in terms of the practicality of the design. The application of the LQG design in the real system will give good results according to the considerations involved in the design of the controller. However, choosing the weights of the design depends on how the user wants the system to behave. For the Robotic Wheelchair System, attention must be taken upon the inclination angle of the wheelchair while in inverse pendulum stage.

Future improvement could take care of the affectivity of the controllers obtained earlier. A possible study could be carried out for developing a derivative action added to the optimal control designs. Improvements of the robustness of the control system are required also.

Another issue is to design a control system with high performance to be able to work for large inclinations inside the nonlinear effect of the system. Digital control study could bring more practical results for the system.

It is been good enjoyable work for doing the project and involving many aspects to control the system and comment on the results.

# 5. References

[1]**SHIROMA Naoji [et al.]** Cooperative Behavior of a Wheeled Inverted Pendulum for Object Transportation [Conference] // IROS 96. - [s.l.] : IEEE, 1996.

**[2]Takahashi Yoshihiko and Tsubouchi Otsushiro** Modern Control Approach for Robotic Wheelchair with Inverse Pendulum Control [Conference] // 5th International Conference on Intelligent Systems Design and Applications (ISDA '05). - [s.l.] : IEEE, 2005.

**[3]Takahashi Yoshihiko, Ishikawa Nobutake and Hagiwara Toshihide** Soft Raising and Lowering of Front Wheels for Inverse Pendulum COntrol Wheel Chair Robot [Conference] // IEEE/RSJ Intl. Conference on Intelligent Robots and Systems. - Las Vegas, Nevada : IEEE, 2003.

**[4]Takahashi Yoshihiko, Machida Shigenori and Ogawa Shinobu** Analysis of front wheel raising and inverse pendulum control of power assist wheel chair robot [Journal]. - 2000.

# 6. Appendix

This appendix will contain the MATLAB codes used. All codes is used under MATLAB R2007b.

List of files:

1) LQR design: proj_lqr.m
2) LQG design: proj_kalman.m
3) H2 design: proj_H2.m
4) H-infinity: proj_H8.m
5) Model Uncertainty: proj_robust.m
6) LQR with Integral Action: proj_LQR_PI.m

All files are included in the CD attached with the report.

### 1) LQR design: proj_lqr.m

```
%term 071
%SE 514 - Optimal Control
%by Mohammad Shahab, King Fahd University of Petroleum & Minerals

%21 JAN 2008

% LQR

clc
clear all

%%%%%%%%%%%%%% Model Parameters



Re=0.84;     %resistance
Mw=6.52;     %wheels mass
L=0.29;      %length between wheels shaft and center of mass
```

```
Kt=0.0239;   %torque constant of DC motor
Jw=0.11;     %intertia of wheels
Kcf=8.78;    %damping between floor and wheels
Kcs=12.3;    %damping of wheel shaft
Mb=84.16;    %mass of wheelchair and person
Jb=29.3;     %inetria of body
rad=0.305;   %radius of wheels
Kg=772;      %gear ratio
Jm=7.0*10^-6;   %inertia of DC motor
g=9.8;       %gravity

%%%%%%%%%%

a1=(Mb*L^2)+Jb+(Kg^2)*Jm;
a2=Mb*rad*L-Jm*Kg^2;
a3=Kcs;
a4=Mb*g*L;
a5=(Kg*Kt)/Re;
b1=(Mb+Mw)*rad^2+Jw+Jm*Kg^2;
b2=Kcs+Kcf;

%%%%%%%%%%

A1=a4*b1/(a1*b1-a2^2);
A2=(a2*a3+a3*b1)/(a1*b1-a2^2);
A3=(a2*b2+a3*b1)/(a1*b1-a2^2);
A4=a2*a4/(a1*b1-a2^2);
A5=(a2*a3+a1*a3)/(a1*b1-a2^2);
A6=(a2*a3+a1*b2)/(a1*b1-a2^2);
B1=(a2*a5+a5*b1)/(a1*b1-a2^2);
B2=(a2*a5+a1*a5)/(a1*b1-a2^2);

%%%%%%%%%% State Space Model

A=[0 0 1 0;0 0 0 1;A1 0 -A2 A3;-A4 0 A5 -A6];

B=[0;0;-B1;B2];

C=[1 -1 0 0;0 0 1 0];

D=[0;0];

sys1=ss(A,B,C,D);

%%%%%%%%%% Initial Conditions

phi0=-0.21;     %initial inclination
th0=0;       %initial wheel rotation
phid0=0;     %initial inclination velocity
thd0=0;      %initial wheel velocity

x0=[phi0;th0;phid0;thd0];

%%%%%%%%%%%% Weighting Matrices
```

```
R=10*eye(1);
Q=1*eye(4);
Q2=C'*(1*eye(2))*C;
Q3=1*[1 0 0 0;0 0 0 0;0 0 0 0;0 0 0 0];
n=[0;0;0;0];

%%%%%%%%%%%  LQR design

[K1,P1,P2,P3]=lqrc(A,B,[Q n;n' R]);

sys_c=ss(A-B*K1,[0;0;0;0],C,D);

%%%%%%%%%%%% Simulation

[y1,t1,x1]=initial(sys_c,x0);
ut=-K1*x1'; %control input

%%%%%%%%%%% Simulation Plots

subplot(3,2,1)
plot(t1,x1(:,1),'-')
title('Inclination Angle')
xlabel('time (sec)')
grid
hold
subplot(3,2,2)
plot(t1,x1(:,2),'-')
title('Rotation Angle')
xlabel('time (sec)')
grid
hold
subplot(3,2,3)
plot(t1,x1(:,3),'-')
title('Incliantion Velocity')
xlabel('time (sec)')
grid
hold
subplot(3,2,4)
plot(t1,x1(:,4),'-')
title('Rotation Velocity')
xlabel('time (sec)')
grid
hold
subplot(3,2,5)
plot(t1,ut,'-')
title('Input Voltage')
xlabel('time (sec)')
grid
hold
```

## 2) LQG design: proj_kalman.m

```
%term 071
%SE 514 - Optimal Control
%by Mohammad Shahab, King Fahd University of Petroleum & Minerals
%21 JAN 2008
%LQG
clc
clear

%%%%%%%%%%%%%% Model Parameters

Re=0.84;     %resistance
Mw=6.52;     %wheels mass
L=0.29;      %length between wheels shaft and center of mass
Kt=0.0239;    %torque constant of DC motor
Jw=0.11;     %intertia of wheels
Kcf=8.78;    %damping between floor and wheels
Kcs=12.3;    %damping of wheel shaft
Mb=84.16;    %mass of wheelchair and person
Jb=29.3;     %inetria of body
rad=0.305;   %radius of wheels
Kg=772;      %gear ratio
Jm=7.0*10^-6;    %inertia of DC motor
g=9.8;       %gravity

%%%%%%%%%%

a1=(Mb*L^2)+Jb+(Kg^2)*Jm;
a2=Mb*rad*L-Jm*Kg^2;
a3=Kcs;
a4=Mb*g*L;
a5=(Kg*Kt)/Re;
b1=(Mb+Mw)*rad^2+Jw+Jm*Kg^2;
b2=Kcs+Kcf;

%%%%%%%%%%

A1=a4*b1/(a1*b1-a2^2);
A2=(a2*a3+a3*b1)/(a1*b1-a2^2);
A3=(a2*b2+a3*b1)/(a1*b1-a2^2);
A4=a2*a4/(a1*b1-a2^2);
A5=(a2*a3+a1*a3)/(a1*b1-a2^2);
A6=(a2*a3+a1*b2)/(a1*b1-a2^2);
B1=(a2*a5+a5*b1)/(a1*b1-a2^2);
B2=(a2*a5+a1*a5)/(a1*b1-a2^2);

%%%%%%%%%%  State Space Model

A=[0 0 1 0;0 0 0 1;A1 0 -A2 A3;-A4 0 A5 -A6];

B=[0;0;-B1;B2];

C=[1 -1 0 0;0 0 1 0];
```

```
D=[0;0];

sys1=ss(A,B,C,D);
Cout=[1 0 0 0];
%%%%%%%%%%

phi0=-0.21;     %initial inclination
th0=0;      %initial wheel rotation
phid0=0;    %initial inclination velocity
thd0=0;     %initial wheel velocity

x0=[phi0;th0;phid0;thd0];

%%%%%%%%%%%% Initial Conditions

R=1*eye(1);
Q=eye(4);
Q2=1*Cout'*Cout;
Q3=1*[0.1 0 0 0;0 0 0 0;0 0 1 0;0 0 0 0];
n=[0;0;0;0];

Bw=[0.09;0.025;0.075;.05];

[K1,P1,P2,P3]=lqrc(A,B,[Q3 n;n' R]);

%%%%%%%% Kalman design

sys2=ss(A,[B Bw],C,[D 0*C*Bw]);

[sys_e,Le,Pe]=kalman(sys2,1,1*eye(2));

Ke=K1;

sys_reg=lqgreg(sys_e,Ke);

sys_c=feedback(sys2,sys_reg,1,[1 2],+1);

%%%%%%%%%%%% Simulation
dt = 0.01;
t = 0:dt:30;   % time samples
wx = wgn(length(t),1,1);

[y1,t1,x1]=lsim(sys_c,[0*wx 0.25*wx],t,[x0;0;0;0;0]);
ut=-Ke*x1(:,5:8)';
current=(ut/Re)';

%%%%%%%%%%% Simulation Plots
subplot(3,2,1)
plot(t1,x1(:,1),'-')
title('Inclination Angle')
xlabel('time (sec)')
grid
```

```
hold
subplot(3,2,2)
plot(t1,x1(:,2),'-')
title('Rotation Angle')
xlabel('time (sec)')
grid
hold
subplot(3,2,3)
plot(t1,x1(:,3),'-')
title('Incliantion Velocity')
xlabel('time (sec)')
grid
hold
subplot(3,2,4)
plot(t1,x1(:,4),'-')
title('Rotation Velocity')
xlabel('time (sec)')
grid
hold
subplot(3,2,5)
plot(t1,current,'-')
title('Current Input (A)')
xlabel('time (sec)')
grid
hold
```